

NUMERICAL SIMULATION OF SHEAR BEHAVIOUR OF REINFORCED HIGH-STRENGTH CONCRETE MEMBERS

S.V. Thilanka Janaka Perera,
Postgraduate student (Saitama University, Japan)
(email: janaka@mtr.civil.saitama-u.ac.jp)
Hiroshi Mutsuyoshi,
Professor (Saitama University, Japan)
(email: mutuyosi@mail.saitama-u.ac.jp)

Abstract

The rapidly increasing use of high-strength concrete (HSC) is outpacing the development of appropriate recommendations for its application. A number of empirical formulae have been proposed for the prediction of the diagonal cracking shear capacity of HSC members. However, these incorporate no explicit consideration of fracture surface roughness or bond stiffness. This paper addresses this key qualitative knowledge on shear behaviour of reinforced high-strength concrete (RHSC) members. Currently, multi-directional fixed crack modeling is being used not only for design but also for maintenance. The diagonal cracking shear strength of RHSC beams, which are greatly affected by both fracture surface roughness and bond stiffness, was simulated using nonlinear finite element (FE) analysis. The test results were compared with predicted strengths using a two dimensional finite element method (2D-FEM). The average of the ratio of tested diagonal cracking shear strength to predicted was 1.04 with a standard deviation of 0.08. The multi-directional fixed crack approach was verified as a reliable structural concrete model in the case of HSC.

Keywords: bond stiffness, fracture surface roughness, high strength concrete, shear

1. Introduction

High-strength concrete (HSC) is being increasingly used in buildings and bridges because it enables the use of smaller cross-sections, longer spans, reduction in girder height and improved durability (Mutsuyoshi et al. 2010). Presently the target compressive strength of concrete easily exceeds 80 MPa. However, the diagonal cracking shear capacity of reinforced high-strength concrete (RHSC) beams does not increase as expected with the increase in the compressive strength of concrete (Perera et al. 2009). Also, an increase in the concrete compressive strength produces an increase in its brittleness, smoothness of shear failure surface, and shrinkage due to self-desiccation at early ages. These limitations have led to some concerns about diagonal shear capacity of HSC beams.

The diagonal cracking shear force in reinforced concrete (RC) members is transferred in various ways. After development of flexural cracks, shear force acting on a cracked section is carried by: 1) the shear resistance of un-cracked concrete in the compression zone; 2) the interlocking action of aggregates along the rough concrete surfaces on each side of the crack; and, 3) the dowel action of the longitudinal reinforcement. For rectangular beams, approximately 50-90% of the vertical shear is carried by aggregate interlocking and un-cracked concrete in the compression zone (Taylor and Brown 1963).

According to past studies, the effect of HSC on shear transfer mechanism is as follows. The shear resistance of un-cracked concrete in the compression zone is reduced due to the brittleness of HSC (Gettu et al. 1990). The crack surface of HSC beams is relatively smooth compared to normal strength concrete (NSC) because cracks penetrate through the aggregate. This smooth crack surface reduces the aggregate interlock and the shear strength of HSC beams (Perera et al. 2010). Also, early-age shrinkage causes deterioration in shear strength in diagonal cracks of reinforced HSC beams. Maruyama et al. (2006) and Perera et al. (2011) detected cracking around reinforcing bars due to early-age shrinkage (autogenous shrinkage) of HSC. From the comparison of self-induced stress in RC prisms with different early-age shrinkages it was concluded that this kind of crack degrades bond stiffness. Therefore, the dowel action of the longitudinal reinforcement is affected by early-age shrinkage. However, there is a gap in existing knowledge as most of the aforementioned studies have been done on concrete with strength of less than 80 MPa due to design limitations (Perera et al. 2009).

A number of empirical formulae have been proposed for the prediction of the diagonal cracking shear capacity of HSC members (Zink 2000, Fujita et al. 2002, Suzuki et al. 2003), but these fail to explicitly consider brittleness, fracture surface roughness, and bond stiffness. This paper's aim is to address this key qualitative knowledge from the perspective of path-dependent mechanistic modeling. Path-dependent constitutive models have been successfully applied to the behavioural simulation of HSC members (Vecchio and Collins 1986, Maekawa et al. 2003). Currently, multi-directional fixed crack modeling is being used not only for design but also in the maintenance

phase of existing infrastructure. This paper discusses the impact of fracture surface roughness and bond stiffness of HSC. The main aim of the work is to accurately predict the shear behavior of RHSC beams using a two dimensional finite element method (2D-FEM).

2. Experimental data on RHSC beams

This section outlines the experimental investigation carried out by Perera et al. (2009, 2010, 2011), where the applicability of the FE framework with integrated path-dependent RC constitutive models was examined. Test variables and material properties are summarized in Table 1. Figure 1 indicates the dimensions and detailing of the specimens. None of the beams have web reinforcement so as to ensure that they fail in shear mode. In the experiment, beams with low and high early-age shrinkage (LA and HA, respectively) were examined.

Table 1: Test variables and beam test results

Beam	f'_c (MPa)	f_t (MPa)	E_c (GPa)	G_F (N/mm)	ε_{sh} ($\times 10^{-6}$)	V_f (kN)	V_c (kN)	V_u (kN)	Failure mode
NSC40	36	3.1	32.1	0.225	-73	17.5	76.5	76.5	DT
HA 100	114	5.2	36.5	0.220	-322	26.5	85.0	85.0	DT
HA 120	138	7.2	39.5	0.229	-412	28	82.5	82.5	DT
LA 120	155	8.3	41.0	0.248	-168	34.5	85.0	120.5	SC
HA 160	183	7.4	43.5	0.250	-511	27.5	75.0	105.5	SC
LA 160	175	8.5	44.7	0.259	-225	35.2	67.0	153.0	SC

f'_c : characteristic compressive strength; f_t : tensile strength of concrete;

G_F : fracture energy in mode I; ε_{sh} : Shrinkage strain in concrete; V_f : Flexural cracking load;

V_c : Shear force at diagonal cracking; V_u : Shear force at failure; DT: Diagonal tension failure;

SC: Shear compression failure.

Note: shear span to depth (a/d) ratio is 4.0; longitudinal tensile reinforcement ratio (ρ_w) is 3.04%.

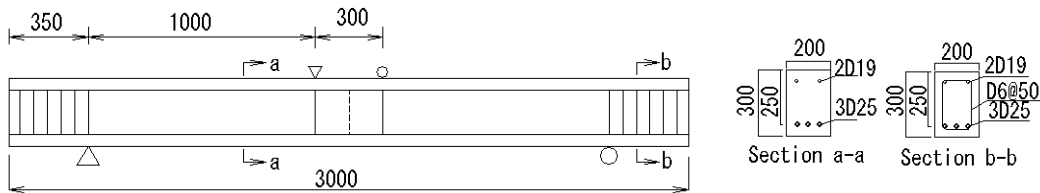


Figure 1: Detail of RC beam (unit: mm)

3. Two-dimensional nonlinear finite element simulation

3.1 Behaviour of shear critical reinforced HSC beams

The beams described above are simulated, in two-dimensional space, using the multi-scale fixed four-way crack model in which the strain-path and time-dependent concrete constitutive models are integrated. This analytical platform has previously been used for the evaluation and understanding of shear critical reinforced NSC and its structural behaviour (Maekawa et al. 2003, An et al. 1998). Provided that the properties of HSC materials can be formulated as appropriate constitutive models with reasonable accuracy, the range of applicability of the platform can be extended based on existing models (Okamura and Maekawa 1991). Using the same analytical framework, Tsuchiya et al. (2002) numerically evaluated the shear performance of RHSC beams with reasonable accuracy. Their paper pointed out the phenomenon whereby the shear failure of RHSC members cannot be addressed solely by changing the compressive strength and presented a number of reasons for this. First, crack surfaces in HSC are characterized by a smoother fracture plane than those in NSC because cracks tend to form through the aggregate particles rather than around them. This can be addressed by reducing the cracked shear transfer resistance of HSC as compared to that of NSC (Bujadham and Maekawa 1992). Second, HSC is characterized by a sudden stress release after cracking, which can be addressed by the tension softening effect. Third, the compression response of HSC is characterized by relatively stiff and brittle response in contrast to that of the NSC. They studied concrete with a compressive strength of 60-70 MPa without silica fume, and used the factorized tensile strength to consider the initial tension caused by autogenous shrinkage (Gebreyouhannes and Maekawa 2011).

3.2 Computational constitutive models of HSC

This section describes the material constitutive models for HSC in tension, shear, and compression that are employed in simulating the RHSC beams. Cracks are expressed by means of a four-way fixed cracking approach based on the active crack method, in which mutual crack-to-crack interaction is considered (Maekawa et al. 2003). A brief outline of the core constitutive models is presented in the subsequent sub-section.

3.2.1 Concrete tension constitutive model

The original tension model by Okamura and Maekawa (1991) which was later enhanced in consideration of high-cycle time-dependent fracturing (Maekawa et al. 2006) is adopted without modification for high-strength plain concrete domain. In the model, the envelope for the post-cracking response is expressed by Eq. (1).

$$\sigma_t \left(\epsilon_c \right) = f_t \left(\frac{\epsilon_{tu}}{\epsilon_c} \right)^c ; \text{ for } \epsilon_c > \epsilon_{tu} \quad (1)$$

$$\epsilon_c = \epsilon_{tot} - \epsilon_{eff_free}$$

where σ_t is the transferred tensile stress, ϵ_{tu} is the crack strain defined equal to $2f_t/E_o$, E_o is the initial stiffness of concrete, ϵ_c is the stress associated strain of concrete after cracking, ϵ_{tot} is the total strain of concrete, ϵ_{eff_free} is the effective stress-free strain of concrete, f_t is the uniaxial tensile strength, and c is a tension softening parameter, which describes the softening stress across the fracture process zone of the concrete. In the multi-directional fixed crack formulation scheme (Maekawa et al. 2003), the value of c depends on the concrete fracturing energy under tension and the sizes of the finite elements (Bazant and Oh 1983). The softening parameter for plain concrete is determined based on the fracture energy balance, which is inversely related to the element size (An et al. 1997) in accordance with Eq. (2) and as illustrated in Figure 2.

$$\frac{G_f}{l} = \int_{\epsilon_{tu}}^{\epsilon_{te}} \sigma_t \left(\epsilon_c \right) d\epsilon_c + 1/4 f_t \epsilon_{tu} \quad (2)$$

where G_f is fracture energy (N/mm), l is element size (mm), ϵ_{tu} is cracking strain, and ϵ_{te} is ultimate tensile strain.

In consideration of the fracture process after cracking, the transient tension model proposed by Soltani (2002) is adopted for the cracked concrete volume in an RC element. The model shows the sudden release of tension that occurs just after crack localization where a low tensile strain field develops. Its applicability to NSC has been validated by experiment (Soltani 2002; Soltani et al. 2003). Even after fracturing advances in plain concrete, tensile stress is spatially transferred over the cracked concrete domain through the bond mechanism of deformed steel and concrete. This post-cracking space-averaged stress-strain relation is generally defined as tension-stiffness. The whole process from brittle tensile softening to stabilized tension transfer through the bond mechanism is shown in Figure 3 (Gebreyouhannes and Maekawa 2011).

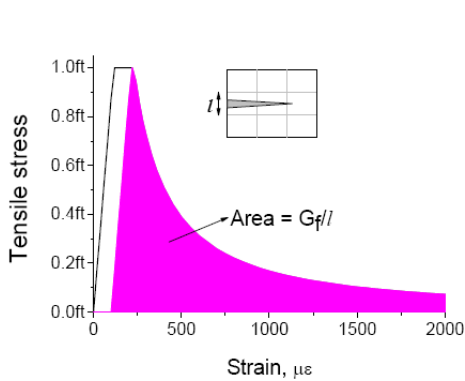


Figure 2: Tension softening of cracked concrete

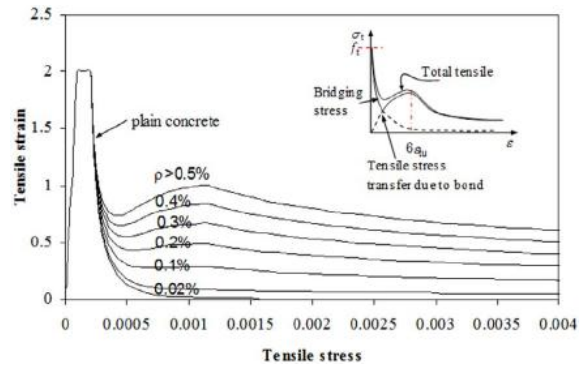


Figure 3: Schematic representation of the transient tension model

3.2.2 Shear model

It is well known that cracks in HSC are characterized by smoother fracture planes. Bujadham and Maekawa (1992) investigated the roughness profile of the crack interface in HSC and proposed a universal shear transfer model based on the concept of contact density (Li et al. 1989). To simulate the RHSC beams under consideration here, this universal shear transfer model is applied to the simulation. The model is based on the integration of local contact forces along a finite crack surface. The transferred shear and confining stresses can be expressed by Eq. (3) as,

$$T = \int_{-\pi/2}^{\pi/2} (N_c \cos\theta + T_c \sin\theta) d\theta$$

$$\sigma = \int_{-\pi/2}^{\pi/2} (N_c \sin\theta + T_c \cos\theta) d\theta \quad (3)$$

where N_c and T_c are the local forces at each contact point along the contact surface in the normal and tangential directions, respectively, and are expressed as Eq. (3a).

$$N_c = K \sigma_{con} A_r \Omega(\theta) d\theta$$

$$T_c = K \tau_{con} A_r \Omega(\theta) d\theta \quad (3a)$$

where A_r represents the area of crack surface per unit projected area and $\Omega(\theta)$ is the density function for defining the geometry of the crack surface (and expressed for HSC as Eq. [3b]).

$$\Omega(\theta) = \frac{5}{6} \exp\left(-21\left(\frac{\theta}{\pi}\right)^2\right) \quad (3b)$$

where $K(\omega)$ represents the proportion of effective contact area and is expressed by the crack width as Eq. (3c).

$$K(\omega) = 1 - \exp\left(1 - \left(\frac{0.5G_{\max}}{\omega}\right)\right) \geq 0 \text{ and } \omega \neq 0 \quad (3c)$$

Since cracks in HSC pass through the aggregate particles, an apparent value of 6 mm is assumed for G_{max} . This is based on an experimental investigation of the crack roughness profile of HSC by Bujadham and Maekawa (1992). The local normal stress, σ_{con} , and the local tangential stress, τ_{con} , are governed by the local deformation of the contact points and are dependent on kinematics of the crack surface. The effects of local anisotropic fracturing and plasticity on the contact points are also rooted in the model and the schematic representation of each is given in Figure 4. The applicability of the model has been verified by extensive experimental results both under single and mixed mode crack kinematics (Bujadham et al. 1992). This highly nonlinear model has been used for RC joints in which discrete crack kinematics prevails. Recently, the applicability of this model has been extended into the smeared crack approach, with an input of crack spacing (Gebreyouhannes and Maekawa 2011).

3.2.3 Compression model

As the main focus of the current study is on the shear failure of RHSC beams prior to yielding of the main reinforcement and concrete compression softening, the time-dependent elasto-plastic and fracture compression model developed for NSC (El-Kashif and Maekawa 2004) is simply adopted without any modification.

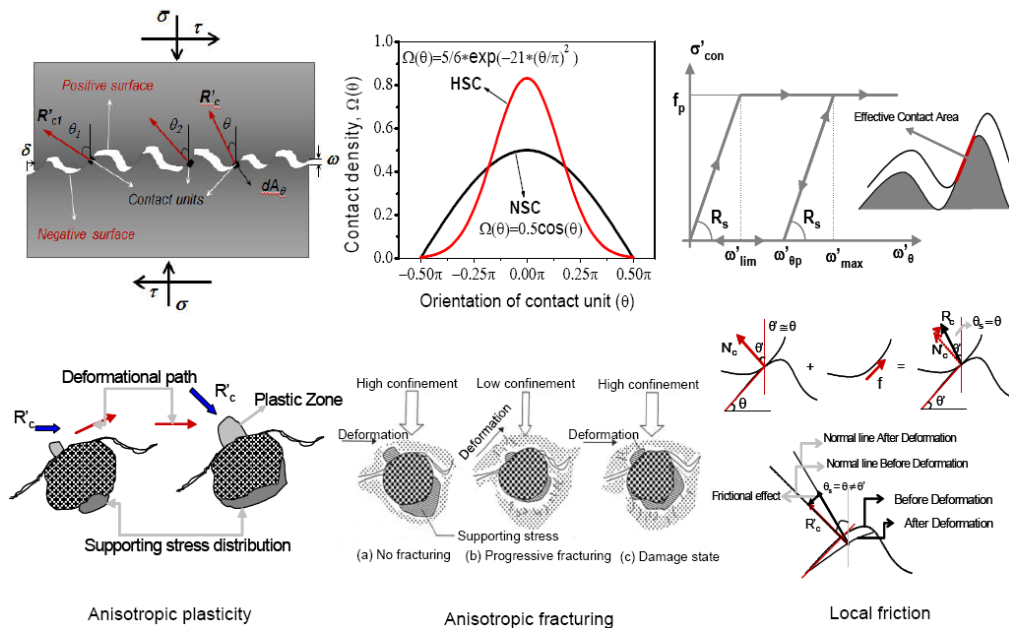


Figure 4: Schematic representation of the universal shear transfer model (Bujadham and Maekawa 1992)

3.3 Finite element modeling

Two-dimensional nonlinear finite element analyses were carried out for the experimental study identified above. The analyses were performed using the multi-directional fixed crack FE frame

work. A typical finite element model representing one of the beams is shown in Figure 5. To capture the post-peak localized response, full two-dimensional models were used for all beams. Rectangular meshes with eight nodes were used. All steel bars were modelled as embedded smeared reinforcement inside the elements. Concrete elements without steel bars were modeled as plain concrete elements characterized by softening behaviour. For each element size, the softening parameter was determined based on the experimentally measured fracture energy. Concrete with steel reinforcement was modeled as RC elements characterized by tension stiffening. The stiffening parameter was set in accordance with the transient tension model (Soltani et al. 2002) using measured values of fracture energy. Loading plates and support bearings were modeled as elastic elements characterized by unyielding behaviour.

The tension model of cracked concrete is explained using Eq. (1) for the case of RC, and c is a parameter controlling the cracking response in the RC domain. In 2D-FEM, the tension stiffening behaviour was modeled as proposed by Perera et al. (2011). That is, near the centre (d distance from the loading point) of RHSC beams, the tension stiffening factor c was taken to be 0.9, while for NSC beams it was 0.4 (Figure 6). However, the softening parameter c of plain concrete was different from that of RC. According to Eq. (2), the softening parameter of HSC was taken to be 10, while for NSC it was 2.

In 2D-FEM, a smeared crack model based on average stress-strain was used to model concrete after cracking (Maekawa et al. 2003). For post-cracking behaviour, the compression and tension model proposed by Maekawa et al. (2003) was used. In the model, to describe the geometry of the crack plane (Figure 4), the crack shear transfer magnification factor (α) was used. Generally, this factor is set to 1.0 for NSC ($f'_c \leq 60$ MPa) and to 0.3-0.5 for HSC ($f'_c \geq 60$ MPa). According to Perera and Mutsuyoshi (2011), the surface roughness of NSC beams was about 14% and 16% greater than that of 114 and 155 MPa beams respectively. Therefore, during the analysis, α was reduced proportionately from $\alpha = 1.0$ to 0.1 as f'_c increased from 38 MPa to 155 MPa (Figure 7).

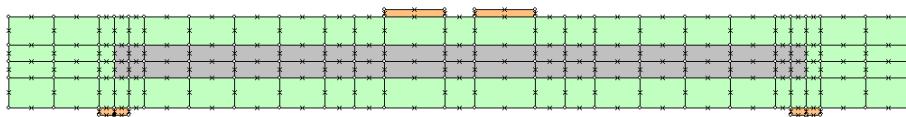


Figure 5: Typical FE model

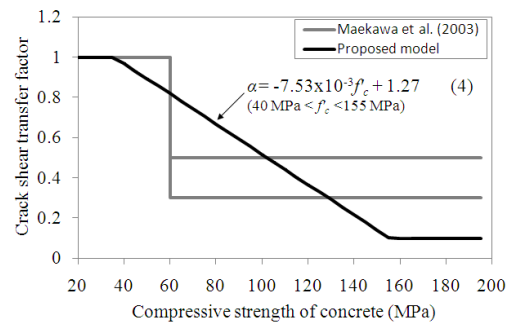
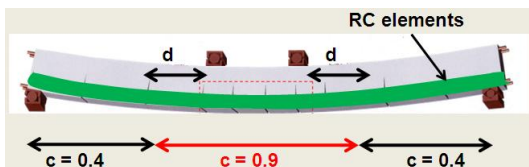


Figure 6: Recommended tension stiffening factors for RHSC beams

Figure 7: A recommended modification to the crack shear transfer factor

4. Comparison of predictions and experimental results

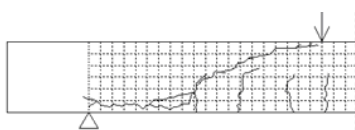
Figure 8 shows a comparison of the experimental and analytical results for NSC40 and HA160 beams. The tensile strength of the HA160 beam was 58% higher compared to that of the NSC40 beam while the load corresponding to the formation of the diagonal shear crack is almost same for both. The ultimate shear capacity in the case of the NSC40 beam was 27% lower than that of the HA160 beam. This is mainly due to the different failure modes observed in the NSC40 and HA160 beams: diagonal tension and shear compression, respectively. The crack patterns of each beam after failure are shown in Figures 8a, b, c, d. As can be seen in Figure 8c and 8d, the formation and localization of diagonal cracking in the HA160 beam was closer to the loading point compared to that of the NSC40 beam. This trend was also observed experimentally. Overall, the behaviour of the beams was predicted quite well.

Table 2 summarizes the ratio of tested loads to predicted loads of flexural cracking, diagonal cracking, and ultimate failure using 2D-FEM. The predicted results show a good correlation with the experimental results. However, the predicted ultimate failure load in the LA120 beam was very conservative compared to the experimental results. This underestimation may be due to unexpected failure mode in the LA120 beam. Furthermore, all in all, the analytical results reasonably replicate the experimental results in term of loads of flexural cracking, diagonal cracking, and ultimate failure.

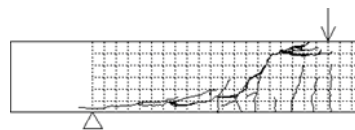
Table 2: Predicted results

Beam	F	D	U
NSC40	1.40	0.99	0.99
HA100	1.20	1.08	1.08
HA120	1.10	1.02	1.02
LA120	1.35	1.05	1.49
HA160	0.93	1.15	1.00
LA160	1.15	0.93	1.49
Average	1.19	1.04	1.18
SD	0.17	0.08	0.24

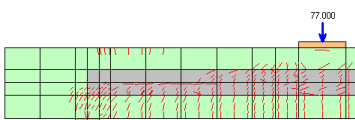
F: $V_f / V_{f-2D-FEM}$; D: $V_c / V_{c-2D-FEM}$; U: $V_u / V_{u-2D-FEM}$; SD : Standard deviation.



a) Actual crack pattern NSC40

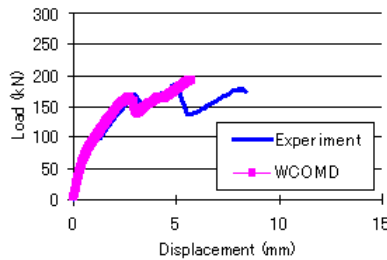
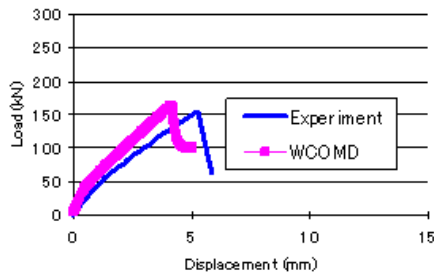


b) Crack pattern HA160



c) Predicted crack pattern NSC40

d) Crack pattern HA160



e) Load versus mid-span deflection NSC40

f) Load versus mid-span deflection HA160

Figure 8: Comparison of experimental and analytical results for beams NSC40 and HA160

5. Conclusions

The shear behaviour of RHSC beams was simulated using a multi-directional fixed crack based model of RC in which appropriate constitutive models for HSC were incorporated. The following conclusions have been drawn from the results:

- I. The effect of fracture surface roughness and bond stiffness in RHSC beams can be addressed according to the suggestions made in this paper.
- II. The average ratio of tested to predicted diagonal cracking shear strength of RC beams using 2D-FEM was 1.04 with a standard deviation of 0.08.
- III. The authors strongly emphasize that accurate measurements of fracture surface roughness and bond stiffness are crucial in assessing the structural performance of RHSC beams with regard to shear.

References

An X, Maekawa K and Okamura H (1997) "Numerical Simulation of Size Effect in Shear Strength of RC Beams", *Journal of Materials, Concrete Structures and Pavements, JSCE*, 35(564): 297-316.

Bazant Z P and Oh B H (1983) "Crack Band Theory for Fracture of Concrete", *Materials and Structures, RILEM*, 16(3): 155-177.

Bujadham B and Maekawa K (1992) "The Universal Model for Stress Transfer Across Cracks in Concrete", *Proceedings of JSCE*, 17(451): 277-287.

Bujadham B, Mishima T and Maekawa K (1992) "Verification of the Universal Stress Transfer Model", *Proceedings of JSCE*, 17(451): 289-300.

El-Kashif K F and Maekawa K (2004) "Time-Dependent Nonlinearity of Compression Softening in Concrete", *Journal of Advanced Concrete Technology*, 2(2): 233-247.

Fujita M, Sato R, Matsumoto K and Takaki Y (2002) "Size Effect on Shear Strength of RC Beams Using HSC without Shear Reinforcement", *Journal of Materials, Concrete Structures and Pavements*, JSCE, 56(711): 161-172 (in Japanese).

Gebreyouhannes E and Maekawa K (2011) "Numerical Simulation on Shear Capacity and Post-Peak Ductility of Reinforced High-Strength Concrete Coupled with Autogenous Shrinkage", *Journal of Advanced Concrete Technology*, 9(1): 73-88.

Gettu R, Bazant Z P and Karr M K (1990) "Fracture Properties and Brittleness of High-Strength Concrete", *ACI Materials Journal*, 87(66): 608-618.

Li B and Maekawa K (1989) "Contact Density Model for the Stress Transfer Across Cracks in Concrete", *Journal of the faculty of Engineering, The University of Tokyo*, XL(1): 9-52.

Maekawa K, Pimanmas A and Okamura H (2003) "*Nonlinear Mechanics of Reinforced Concrete*" Spon Press.

Maekawa K, Toongoenthong K, Gebreyouhannes E and Kishi T (2006) "Direct Path-Integral Scheme for Fatigue Simulation of Reinforced Concrete in Shear", *Journal of Advanced Concrete Technology*, 4(1): 159-177.

Maruyama I, Kameta S, Suzuki M and Sato R (2006) "Cracking of High-Strength Concrete Around Deformed Reinforcing Bar Due to Shrinkage", *Int. RILEM-JCI Seminar on Concrete Durability and Service Life Planning*, edited by K, Kovler, RILEM Publications S.A.R.L., Ein-Bokek, Israel, 104-111.

Mustuyoshi H, Ichinomiya T, Sakurada M and Perera S V T J (2010) "High-Strength Concrete for Prestressed Concrete Structures", *CPI Trade Journal for the Concrete Industry*, August 2010, 42-46.

Okamura H and Maekawa K (1991) "Nonlinear Analysis and Constitutive Models of Reinforced Concrete", *Gihodo-Shuppan*, Tokyo, Japan.

Perera S V T J and Mutsuyoshi H (2011) "Shear Behaviour of Reinforced High-Strength Concrete Beams", *ACI Structural Journal*, (accepted for publication).

Perera S V T J, Mutsuyoshi H, Nyunt N M and Watanabe H (2011) “Tension Stiffening of Reinforced High-Strength Concrete Tension Members”, *Proc. of Japan Concrete Institute (JCI)*, 33(2): 685-690.

Perera S V T J, Mutsuyoshi H, Takeda R and Asamoto S (2010) “Shear Behaviour of High-Strength Concrete Beams”, *Proc. of Japan Concrete Institute (JCI)*, 32(2): 685-690.

Perera S V T J, Quang L H, Mutsuyoshi H and Minh H (2009) “Shear Behaviour of Reinforced Concrete Beams Using High-Strength Concrete”, *Proc. of Japan Concrete Institute (JCI)*, 31(2): 589-594.

Soltani M (2002) “Micro-Computational Approach to Post-Cracking Constitutive Laws of Reinforced Concrete and Application to Nonlinear Finite Element Analysis”, PhD Thesis, The University of Tokyo.

Soltani M, An X and Maekawa K (2003) “Computational Model for Post Cracking Analysis of RC membrane Element Based on Local Stress-Strain Characteristics”, *Engineering Structures*, 25(8): 993-1007.

Suzuki M, Akiyama M, Wang W L, Sato M, Maeda N and Fujisawa Y (2003) “Shear Strength of RC Beams without Stirrups Using High-Strength Concrete of Compressive Strength Ranging to 130 MPa”, *Journal of Materials, Concrete Structures and Pavements, JSCE*, 60(739): 75-91 (in Japanese).

Taylor R and Brown R S (1963) “The Effect of the Type of Aggregate on the Diagonal Cracking of Concrete Beams”, *Magazine of Concrete Research*, July 1963.

Tsuchiya S, Mishima T and Maekawa K (2002) “Shear Failure and numerical Evaluation of RC Beam Members with High-Strength Materials”, *Journal of Materials, Concrete Structures and Pavements, JSCE*, 54(697): 65-84 (in Japanese).

Vecchio F J and Collins M P (1986) “The Modified Compression Field Theory for Reinforced Concrete Elements Subjected to Shear”, *ACI Journal Proceedings*, 83(2), March-April 1986, 219-321.

Zink K (2000) “Diagonal Shear Cracking in Slender Concrete Beams”, *LACER No. 5*, University of Leipzig, 305-332.